UNITED STATES DEPARTMENT OF THE INTERIOR
U.S. GEOLOGICAL SURVEY

Heat capacities of synthetic grossular ($Ca_3Al_2Si_3O_{12}$), macro-crystals of magnesite ($(Mg_{0.991}Fe_{0.005}Ca_{0.003}Mn_{0.001})CO_3$), high-temperature superconductors $YBa_2Cu_3O_{6+x}$ and $BiCaSrCu_2O_{6+x}$, and type 321 stainless steel[1].

by

Richard A. Robie[2] and Bruce S. Hemingway[2]

Open file Report 94-223

---

1. This report is preliminary and has not been edited or reviewed for conformity with U.S. Geological Survey editorial standards.
2. MS 959, U.S. Geological Survey, Reston, VA 22092

Introduction

During the past 20 years, we have measured the low-temperature heat capacity of a number of materials which had only incidental relationships to our main studies, that of determining the thermodynamic properties of minerals. While these data do not warrant a formal report of themselves they are of high quality and since someday they may well be useful to other investigators, we feel they should be recorded in a manner such that the data can be accessed without too much difficulty. The data are presented here with only a limited discussion.

Grossular

There are at least 3 different calorimetric values for the entropy of grossular in the mineralogical literature. The first, due to Westrum et al. (1979) was based upon measurements of a natural specimen from Thetford, Quebec and gave a value for S°_{298}, after a significant correction for impurities, of 254.6 $\pm$ 0.8 $J \cdot mol^{-1} \cdot K^{-1}$. The second value, also determined from measurements on a natural mineral sample, 256.5 $\pm$ 1.3 $J \cdot mol^{-1} \cdot K^{-1}$ was obtained by Kolesnik et al. (1979). Haselton and Westrum (1980) studied a synthetic grossular prepared at 25 kbar and 1673 K. Their results yielded S°_{298} = 260.12 $\pm$ 0.5 $J \cdot mol^{-1} \cdot K^{-1}$, significantly greater than either of the previous values.

In order to reassure ourselves that the entropy of synthetic grossular ($Ca_3Al_2Si_3O_{12}$) was indeed that as given by Haselton and Westrum (1980) and also to check that there was no systematic difference in the values of C°_p measured with our calorimetric system and those measured in the calorimetry laboratory at the University of Michigan (also see Anovitz et al., 1987) we remeasured the heat capacity of the Haselton-Westrum synthetic grossular. The sample mass available was 9.2193 g and was smaller than we would have desired. The sample was only 4.4% of the gross heat capacity at 20 K and 19.3% at 315 K.

Our experimental results are listed in Table 1. Because of the very unfavorable ratio of sample C_p/[(sample + calorimeter)C_p] we adopted the Haselton-Westrum value for S°_{20} (0.238 $J \cdot mol^{-1} \cdot K^{-1}$) which we added to the value of $\int_{20}^{298.15} C_p/TdT$ calculated from our measurements to get $S^\circ_{298.15}$. Our value for the entropy of grossular at 298.15 K obtained this way is 259.9 $\pm$ 1.0 $J \cdot mol^{-1} \cdot K^{-1}$ which is 0.08 percent smaller than that reported by Haselton and Westrum (1980). Between 100 and 300 K, our smoothed values of C_p differ from those of Haselton and Westrum (1980) by +0.7% at 100K to -0.2 percent at 300 K. A table of smoothed thermodynamic properties for grossular calculated from our data, as described above, is given in Table 2.

The conclusions we draw from our measurements are as follows: the measurements on the natural material required rather significant corrections to extract $S^\circ_{298.15}$ for ideal grossular and are thus suspect; our calorimetric system and that at the University of Michigan yield essentially the same value for S°_{298} for the synthetic grossular; and, the obvious one, that the use of a small sample merely leads to a greater scatter of the data, not to any systematic error, except at very low temperatures where the uncertainty is very large.

Magnesite $(Mg_{0.991}Fe_{0.005}Ca_{0.003}Mn_{0.001})CO_3$ crystals

Fornaseri (1941) described large crystals of magnesite from Serra das Eugas (Bahia), Brazil, which had the composition $(Mg_{0.980}Ca_{0.006}Fe_{0.007}Mn_{0.001})CO_3$. A group of large glass clear magnesite crystals which had been collected by U.S. Geological Survey geologists in the Serra das Eugas area of Brazil was located in a laboratory undergoing renovation. This material fitted the description of the crystals described by Fornaseri (1941) and a microprobe analysis of this material (see Table 3) gave a composition of $(Mg_{0.991}Fe_{0.005}Ca_{0.003}Mn_{0.001})CO_3$.

The availability of these large glass clear crystals suggested the possibility of comparing their heat capacity with that of finely crystalline (10 to 70 μm) synthetic magnesite measured by Hemingway et al. (1977) in this laboratory to determine whether there was a surface energy contribution to the measured heat capacity of the fine grained magnesite sample (e.g., Giauque and Archibald, 1937); and to provide a somewhat more quantitative look at the effect of small amounts of transition metal ion impurities on the heat capacities of a non-magnetic solid at very low temperatures. The heat capacity measurements were performed on a 51.156 g (mass) sample of rhombohedral cleavage fragments which ranged from 3 to 15 mm on edge. The results of our measurements are reported in Table 4 as specific heats (ie., units are $J \cdot g^{-1} \cdot K^{-1}$).

Between 70 and 300 K, the values for the heat capacity of the large natural crystals and the values reported earlier by Hemingway et al. (1977) for synthetic $MgCO_3$ agree to within +0.2 to -0.6 percent. The earlier measurements were made with a different calorimeter and temperature scale. Below 70 K, the specific heat of the large crystals exceeds that of the synthetic micro-crystals by up to 4.1 percent, near 40 K. This presumably arises mainly from the substitutions of Fe^{+2} for Mg^{+2}. At 40 K, for example, the molar heat capacity of $FeCO_3$ is 10.8 times greater than that of $MgCO_3$. Smoothed values of the thermodynamic properties of $MgCO_3$ calculated from our corrected experimental data are listed in Table 5. The entropy at 298.15 K, 64.98 $J \cdot mol^{-1} \cdot K^{-1}$, is 0.2 percent smaller than the value reported by Hemingway et al. (1977). These two values are in excellent agreement.

The only previous measurements of C_p° for magnesite above $\approx$350 K are the unpublished heat content data of C.H. Shomate, up to 743 K, and are referred to by Kelley (1960). We also measured the heat capacity of the magnesite crystals over the range 339 to 676 K by differential scanning calorimeter. The results are listed in Table 6.

$YBa_2Cu_3O_{6+x}$

In March, 1988, we were asked by Dr. C.K. Chiang (NIST, National Institute of Standards and Technology) if we would measure the low-temperature heat capacity of a sample of the recently discovered 90 K superconductor $YBa_2Cu_3O_{6+x}$ that he had prepared and upon which he had made magnetic susceptibility measurements. Because of the excitement in the scientific world about these new materials and because of the importance of C_p° measurements for understanding the nature and in determining the extent of the normal → superconducting transition within the sample volume, we readily agreed and the measurements were accordingly made in March, 1988, and an unpublished report was submitted in April of 1988.

The ceramic superconductor, $YBa_2Cu_3O_{6+x}$ with x nominally 0.9 was prepared by solid state reaction. The starting material was a stoichiometric mixture of $BaCO_3$, Y_2O_3 and CuO. The mixture was first sintered at 800°C for 12 hours with one regrinding and then it was fired at 940°C for 48 hours in air. The product then was cooled slowly to 750°C in flowing oxygen and held for 7 hours, cooled further to and held at 400°C for 12 hours. The furnace was turned off and the ceramic allowed to cool slowly in the furnace to about 150°C before it was removed from the furnace. The sample was shown by ac susceptibility measurement to become superconducting at ~92 K.

The heat capacity of nominal $YBa_2Cu_3O_{6.9}$ was measured between 8.2 and 330.6 K using an adiabatically shielded calorimeter with intermittent heating. The sample weight was 20.267 g. It was corrected for buoyancy using a density of 6.36 $g \cdot cm^{-3}$ calculated from the unit cell parameters. It was sealed in the calorimeter under a pressure of 5.1 kPa of pure helium gas in order to promote rapid thermal equilibrium between the sample and calorimeter. The heat capacity of the sample corresponded to 16 percent of the gross measured heat capacity (sample + calorimeter) at 10 K, increasing to 24 percent at 22 K and then decreasing to 19.5 percent at 330 K. Our experimental data are listed in their chronological order of measurement in Table 7 and are shown graphically in Figure 1.

Our C_p° data have an accuracy of ±0.2 percent above 25 K. The accuracy decreases below 25 K to approximately 10 percent at 10 K. Part of the scatter in the data arises from the small amount of sample available leading to an unfavorable ratio of C(sample)/ C(container). In the region of the transitions, measurements made with small temperature rises will have additional scatter because of the reduced precision in the measurement of ΔT (approximately .001 K above 50 K) because of the fixed sensitivity of the platinum thermometer.

Our measurements in the neighborhood of the transition from the normal to the superconducting state are shown in Figure 2. Some measurements *overlapped* the transition region, those measurements for which the initial rating period of a heat capacity measurement was made with the sample in the superconducting state but for which the final rating period the sample was in the normal state. These data are perfectly good finite enthalpy increments but are not true differential heat capacities (ie. dH/dT). These values are indicated by asterisks in Table 7.

If we extrapolate the two heat-capacity curves from above and below the normal to superconducting transition in Figure 2 to the same temperature, we get $\Delta C_p \approx 2.2 \pm 0.3$ $J \cdot K^{-1} \cdot mol^{-1}$. We assign 88.0 ± 0.5 K as the transition temperature (T_c) for our sample. T_c for our sample is clearly less than the 90 to 92 K reported by some other investigators.

Our value for ΔC_p is smaller than that for $YBa_2Cu_3O_{6.5}$ given by Shaviv et al. (1987) and lies in the middle of the range of values obtained by Lægreid et al. (1987) on samples whose oxygen contents were not specified. Lægreid et al. (1987) also reported a transition at 220 K, whose magnitude is dependent upon the size of the C_p°-jump at ≈ 90 K. Our measurements in the range 200 to 250 K, made at 5 K increments, show *no evidence* for such a transition in our sample. However, there is a transition in CuO at about this temperature (Hu and Johnston, 1953).

After completing the measurements of series 7 (Table 7) the calorimeter was cooled to 55 K and a new series of measurements made at 5 K intervals up to 85 K. These measurements revealed the existence of additional anomalous behavior in C_p° of our sample and the data of series 9 and 10 were then made in order to examine the behavior of C_p° in

this temperature range. Series 9 and 10 clearly show anomalies in C_p° at $\approx$58.5 K and a more pronounced anomaly with a maximum in C_p° at 68.0 K (see Figure 2). We do not know the cause of these C_p° maxima nor whether they are unique to our sample of $YBa_2Cu_3O_{6.9}$. Small changes in the slope of the ac susceptibility curve for this sample (Chiang, written communication, 1988) occur near 58 and 68 K and may be related to the heat capacity anomalies. We considered the possibility that these thermal effects were an artifact of the calorimeter, but since we have never observed this behavior with other materials, we concluded that it was a real feature of our sample. They do not appear to have been observed in previous studies of the heat capacity. In this respect, we note that Cava et al. (1987a) report the existence of a phase of composition $YBa_2Cu_3O_{6.6\text{-}6.7}$ which becomes a bulk superconductor at 60 K. The $YBa_2Cu_3O_{6+x}$ phase is only superconducting for the composition range $0.4 \geq x \leq 0.97$, see for example Loram et al. (1993). From their curve of T_c versus x and our observed value for T_c of 88 K, we conclude that the composition of our sample was closer to $YBa_2Cu_3O_{6.8}$ than to its nominal composition of $YBa_2Cu_3O_{6.9}$. We also point out that none of the phases used to prepare our sample, Y_2O_3, $BaCO_3$, and CuO, have transitions in C_p° in the temperature range 50-90 K. The small anomaly in C_p° for CuO occurs at $\approx$ 220 K, as previously noted. If the C_p° maxima at 58.5 and 68.0 K are due to the presence in our sample of a second Y-Ba-Cu-O phase, it must have a rather large C_p° anomaly. The anomaly in C_p° that one observes at 68 K is already an order of magnitude larger than that arising from the superconductor-normal C_p° jump at $\approx$ 88 K.

After our C_p° measurements had been completed and because of the low value of the superconducting transition temperature ($T_c \approx$ 88 K) we made an x-ray diffraction study of the sample. The diffractometer tracing agreed well with the indexed d-spacings given by Cava et al. (1987b). There were, however, several additional weak lines (relative intensity of 3/100) that are not in Cava et al.'s (1987b) pattern. These additional lines do not correspond to CuO, Y_2O_3, $BaCO_3$, (ie., the starting materials) or to $BaCuO_2$, but may possibly arise from a few percent of the phase Ba_2CuO_3 whose 4 strongest lines are close to the positions of our "extra lines."

At temperatures below $\approx$ 3 K almost all samples of $YBa_2Cu_3O_{6+x}$ exhibit an upturn in C_p°/T with decreasing temperature. This is caused by a Schottky-type anomaly (see discussion by Phillips et al., 1992). Thus in the absence of C_p° measurements on our sample between 0.1 and 10 K, we cannot make a proper extrapolation of C_p°/T to 0 K and consequently we cannot evaluate $\int_0^{10} C_p^\circ/T dT = S_{10}^\circ$. Accordingly we report only the value

$S_{298}^\circ - S_{10}^\circ = 324.9 \pm 0.7\ J \cdot K^{-1} \cdot mol^{-1}$.

$BiCaSrCu_2O_{6+x}$

In June of 1988, we received a second high-temperature superconductor from Dr. C. K. Chiang (NIST). The superconducting transition was reported to be at about 110 K. Measurements of the heat capacity were made from 8 to 329 K with the results reported to Dr. Chiang in July of 1988. There was no clear-cut evidence for a jump in heat capacity in the region near 110 K. Although the sample showed superconductivity, the heat-capacity data demonstrated that superconductivity was not a property of the bulk sample and,

therefore, that the sample was heterogeneous. Further characterization of this sample was considered unwarranted. Our experimental heat-capacity values are listed in Table 8 and the results are shown in Figure 3. The sample was 35.0396 g and was sealed in the calorimeter under a pressure of 5 kPa of pure helium gas. The sample represented 53, 29, and 33 per cent of the total heat capacity measured at 10, 100, and 300 K, respectively.

Type 321 stainless steel

The hollow metal o-rings which were initially used to seal our low-temperature calorimeters were fabricated from type 321 stainless steel. In order to make corrections (arising from the difference in the weights of different o-rings) to the heat capacity of the empty sample container, and also to investigate the possibility that there is a transformation in 321 type stainless steel and consequently an anomalous heat effect associated with the o-rings made from this alloy, we measured the specific heat of a 101.541 gram sample of type 321 stainless steel between 53.6 and 351.6 K. The results of these measurements are given in Table 9. We found no thermal signature for a low-temperature transition in the strain-free material within the stated temperature region.

References

Anovitz, L.M., Hemingway, B.S., Westrum, E.F., Jr., Metz, G.W., and Essene, E.J., 1987, Heat capacity measurements for cryolite (Na_3AlF_6) and reactions in the system Na-Fe-Al-Si-O-F. Geochemica et Cosmochimica Acta, v. 51, p. 3087-3103.

Cava, R.J., Batlogg, B., Chen, C.H., Rietman, E.A., Zahurak, S.M., and Werder, D., 1987a, Oxygen stoichiometry, superconductivity and normal-state properties of $YBa_2Cu_3O_{7-\delta}$. Nature, v. 329, p. 423-425.

Cava, R.J. Batlogg, R., van Dover, R.B., Murphy, D.W., Sunshine, S., Siegrist, T., Remeika, J.P., Rietman, E.A., Zahurak, S., and Espinosa, G.P., 1987b, Bulk superconductivity in single-phase oxygen-deficient perovskite $Ba_2YCu_3O_{9-\delta}$. Physical Review Letters, v. 58, p. 1676-1679.

Fornaseri, M. (1941), Magnesite di Serra das Eugas (Bahia, Brazil): Rendiconti della Societa mineralogica Italiana, v. 1, p. 60-65.

Giauque, W.F. and Archibald, R.C., 1937, The entropy of water from the third law of thermodynamics. The dissociation pressure and calorimetric heat of the reaction $Mg(OH)_2 = MgO + H_2O$. The heat capacities of $Mg(OH)_2$ and MgO from 20° to 300° K: Journal of the American Chemical Society, v. 59, p. 391-399.

Haselton, H.T., Jr., and Westrum, E.F., Jr., 1980, Low-temperature heat capacities of synthetic pyrope, grossular, and $pyrope_{60}$ $grossular_{40}$: Geochemica et Cosmochimica Acta., v. 44, p. 701-709.

Hemingway, B.S., Robie, R.A., Fisher, J.R. and Wilson, W.H. (1977), Heat capacities of gibbsite, Al $(OH)_3$, between 13 and 480 K and magnesite between 13 and 380 K and their standard entropies at 298.15 K, and the heat capacity of Calorimetry Conference benzoic acid between 12 and 316 K. Journal of Research, U.S. Geological Survey, v. 5, p. 797-806.

Hu, J.-H. and Johnston, H.L., 1953, Low temperature heat capacities of inorganic solids. XVI. Heat capacity of cupric oxide from 15 to 300° K. Journal of the American Chemical Society, v. 75, p. 2471-2473.

Kelley, K.K. (1960), Contributions to the data on theoretical metallurgy XIII. High-temperature heat-capacity, and entropy data for the elements and inorganic compounds: U.S. Bureau of Mines Bulletin 584, 232 p.

Kolelsnik, Y.N., Nogteva, V.V., Arkhipenko, D.K., and Paukov, I.Y., 1979, Thermodynamics of pyrope-grossular solid solutions and the specific heat of grossular. Geochemistry International 1979, p. 57-64.

Lægreid, T., Fossheim, K. Sandvold, E., and Julsrud, S., 1987, Specific heat anomaly at 220 K connected with superconductivity at 90 K in ceramic $YBa_2Cu_3O_{7-\delta}$: Nature, v. 330, p. 637-638.

Loram, J.W., Mirza, K.A., Cooper, J.R., and Liang, W.Y., 1993, Electronic specific heat of $YBa_2Cu_3O_{6+x}$ from 1.8 to 300 K. Physical Review Letters, v. 71, p. 1740-1743.

Phillips, N.E., Fisher, R.A., and Gordon, J.E., 1992, in Brewer, D.F. ed., The specific heat of high-T_c superconductors. Progress in Low Temperature Physics, v. XIII, Chpt. 5, p. 267-357, Elsevier.

Shaviv, R., Westrum, E.F., Jr., Sayer, M., Yu, X., Brown, R.J.C., Heyding, R.D., and Weir, R.D., 1987, Specific heat of a high-T_c perovskite superconductor $YBa_2Cu_3O_{8-\delta}$: Journal of Chemical Physics, v. 87, p. 5040-5041.

Westrum, E.F., Jr., Essene, E.J., and Perkins, D., III, 1979, Thermophysical properties of the garnet, grossular ($Ca_3Al_2Si_3O_{12}$): Journal of Chemical Thermodynamics, v. 11, p. 57-66.

Table 1. Experimental molar heat capacities of synthetic grossular ($Ca_3Al_2Si_3O_{12}$). Formula weight = 450.455 g.

Temp. K	Heat Capacity $J \cdot mol^{-1} \cdot K^{-1}$	Temp. K	Heat Capacity $J \cdot mol^{-1} \cdot K^{-1}$
Series 1		Series 2 (cont.)	
301.27	333.1	118.23	117.4
305.99	339.2	123.84	126.7
310.80	341.2	129.41	136.0
315.66	344.7	134.93	145.4
320.54	348.6	140.41	154.6
		145.85	163.1
Series 2		151.26	171.3
10.13	0.238	156.63	179.4
11.79	0.240	161.99	187.0
12.94	0.400	167.32	194.4
14.56	0.591	172.63	201.3
16.21	0.709	177.92	208.7
18.02	0.919	183.19	216.0
20.02	1.18	188.44	222.8
22.22	1.39	193.68	229.5
24.67	1.81	198.89	236.1
27.40	2.62	204.09	242.8
30.43	4.98	209.27	248.5
33.87	5.47	214.44	254.0
37.74	8.60	219.60	260.5
42.01	10.19	224.77	266.2
46.81	12.57	229.94	271.7
52.16	18.19	235.12	276.6
58.05	30.51	240.28	281.4
64.35	35.74	245.45	286.7
70.80	39.91	250.61	291.5
77.14	53.22	255.77	296.1
83.22	63.39	260.92	300.6
89.20	70.69	266.10	305.4
95.14	78.40	271.29	310.6
101.03	88.75	276.45	315.1
106.83	100.2	281.57	320.0
112.56	109.3	286.66	324.8
		291.73	328.8

Table 2. Standard molar thermodynamic properties of synthetic grossular ($Ca_3Al_2Si_3O_{12}$). Formula weight = 450.455 g·mol^{-1}.

Temp.	Heat capacity	Entropy	Enthalpy function	Gibbs energy function
T	C°_p	$S^\circ_T - S^\circ_0$	$(H^\circ_T - H^\circ_0)/T$	$-(G^\circ_T - H^\circ_0)/T$
Kelvin	J·mol^{-1}·K^{-1}			
5	0.013	0.004	0.003	0.001
10	0.171	0.029	0.022	0.007
15	0.29	0.092	0.068	0.024
20	0.80	0.24	0.18	0.057
25	1.72	0.51	0.39	0.12
30	3.91	0.99	0.77	0.22
35	6.28	1.77	1.39	0.38
40	8.73	2.78	2.16	0.62
45	11.11	3.94	3.02	0.92
50	14.92	5.29	4.00	1.29
60	26.85	9.00	6.76	2.24
70	40.65	14.17	10.61	3.56
80	55.77	20.57	15.29	5.28
90	72.01	28.07	20.69	7.38
100	88.37	36.51	26.64	9.87
110	104.7	45.69	32.99	12.70
120	121.0	55.50	39.64	15.85
130	137.2	65.82	46.52	19.30
140	153.3	76.58	53.58	23.00
150	168.9	87.69	60.75	26.94
160	183.8	99.07	67.98	31.10
170	198.1	110.6	75.22	35.43
180	211.8	122.4	82.43	39.94
190	224.9	134.2	89.58	44.59
200	237.4	146.0	96.66	49.36
210	249.3	157.9	103.6	54.25
220	260.5	169.8	110.5	59.23
230	271.2	181.6	117.3	64.29
240	281.4	193.3	123.9	69.42
250	291.1	205.0	130.4	74.61
260	300.4	216.6	136.8	79.85
270	309.2	228.1	143.0	85.13
280	317.8	239.5	149.1	90.44
290	326.0	250.8	155.0	95.78
300	334.0	262.0	160.9	101.1
310	341.9	273.1	166.6	106.5
320	349.6	284.1	172.2	111.9
273.15	312.0	231.7	144.9	86.80
298.15	332.6	259.9	159.8	100.1

Table 3. Microprobe analyses of large glass clear crystals of magnesite from Serra das Eugas (Bahia), Brazil.

Run	MgO	CaO	FeO	MnO	ZnO	SrO	Total
1	46.2	0.21	0.41	0.06	0.00	0.02	46.9
2	45.6	0.19	0.44	0.04	0.01	0.01	46.3
3	45.8	0.20	0.42	0.07	0.00	0.00	46.5
4	45.8	0.21	0.39	0.08	0.00	0.00	46.5
5	45.7	0.19	0.39	0.06	0.00	0.00	46.3
6	45.8	0.20	0.41	0.07	0.00	0.03	46.5
7	45.9	0.21	0.46	0.04	0.00	0.00	46.6
8	45.6	0.20	0.44	0.08	0.02	0.01	46.4
9	45.6	0.21	0.44	0.09	0.00	0.00	46.3
10	46.0	0.19	0.38	0.05	0.00	0.01	46.6
11	46.0	0.21	0.41	0.05	0.01	0.01	46.7
12	45.4	0.21	0.45	0.10	0.00	0.00	46.2
13	45.4	0.20	0.41	0.08	0.00	0.00	46.1
14	45.7	0.20	0.43	0.06	0.02	0.01	46.5
15	45.9	0.18	0.35	0.10	0.01	0.03	46.5
16	45.5	0.19	0.43	0.06	0.00	0.00	46.2
17	45.6	0.20	0.47	0.10	0.00	0.00	46.4
18	45.3	0.20	0.40	0.06	0.00	0.00	46.0
19	45.3	0.20	0.42	0.07	0.00	0.00	46.0
20	45.5	0.20	0.42	0.06	0.00	0.00	46.2
21	45.6	0.19	0.45	0.05	0.00	0.03	46.3
AVE	45.7	0.2	0.4	0.1	0.0	0.0	46.4

Standards: CDOS, CDOS, CSIG, CRAP, OXGH, CSTR, respectively for the elements listed above.

Operating conditions:

Accel. Volt. = 15 KV
Beam = 0.1 μA, focussed
Count times = 20/10 sec. Pk/Bkg
Bkgd meas. = Offsets

Table 4. Experimental specific heats of $(Mg_{0.991}Fe_{0.005}Ca_{0.003}Mn_{0.001})CO_3$ corrected for curvature.

Temp. K	Heat capacity $J \cdot g^{-1} \cdot K^{-1}$	Temp. K	Heat capacity $J \cdot g^{-1} \cdot K^{-1}$	Temp. K	Heat capacity $J \cdot g^{-1} \cdot K^{-1}$
Series 1		Series 3		Series 4	
303.15	0.9072	54.60	0.0713	185.93	0.6368
307.66	0.9150	59.16	0.0896	190.71	0.6510
312.65	0.9239	63.24	0.1073	195.64	0.6654
317.67	0.9330	67.79	0.1285	200.68	0.6797
322.82	0.9425	73.16	0.1547	205.63	0.6932
327.97	0.9512	78.37	0.1812	210.60	0.7069
333.11	0.9613	83.58	0.2080	215.61	0.7195
338.25	0.9684	88.78	0.2351	220.67	0.7321
343.38	0.9764	93.93	0.2619	225.83	0.7448
		99.01	0.2879	231.15	0.7578
Series 2		104.00	0.3133	236.59	0.7706
		108.92	0.3375	242.08	0.7830
8.25	0.0000	113.77	0.3609	247.62	0.7955
9.34	0.0001	118.56	0.3834	253.20	0.8077
10.36	0.0001	123.30	0.4049	256.79	0.8198
11.51	0.0002	127.98	0.4259		
12.90	0.0004	132.61	0.4461	Series 5	
14.36	0.0007	137.20	0.4651		
15.98	0.0010	141.76	0.4834	255.65	0.8122
17.79	0.0015	146.27	0.5014	261.13	0.8242
19.79	0.0021	150.76	0.5189	266.34	0.8354
21.98	0.0030	155.22	0.5348	271.57	0.8464
24.43	0.0043	159.65	0.5506	276.93	0.8569
27.14	0.0062	164.06	0.5659	282.27	0.8680
30.17	0.0092	168.44	0.5808	287.60	0.8787
33.57	0.0138	172.80	0.5955	292.92	0.8888
37.37	0.0206	177.16	0.6097	298.23	0.8986
41.64	0.0302	181.51	0.6231	303.52	0.9083
46.43	0.0432			308.79	0.9179
51.78	0.0607			314.07	0.9273
57.73	0.0841				
63.95	0.1107				

Table 5. Standard molar thermodynamic properties of magnesite.

Temp.	Heat capacity	Entropy	Enthalpy function	Gibbs energy function
T	C_p°	$S_T^\circ - S_0^\circ$	$(H_T^\circ - H_0^\circ)/T$	$-(G_T^\circ - H_0^\circ)/T$
Kelvin		$J \cdot mol^{-1} \cdot K^{-1}$		
25	0.393	0.061	0.055	0.006
30	0.764	0.162	0.140	0.023
35	1.37	0.322	0.269	0.053
40	2.21	0.557	0.456	0.101
45	3.30	0.878	0.710	0.168
50	4.61	1.29	1.03	0.259
60	7.86	2.41	1.89	0.519
70	11.73	3.90	3.01	0.891
80	15.95	5.74	4.36	1.28
90	20.31	7.87	5.89	1.98
100	24.65	10.24	7.55	2.69
110	28.85	12.79	9.30	3.49
120	32.85	15.47	11.10	4.37
130	36.62	18.25	12.92	5.33
140	40.15	21.09	14.74	6.38
150	43.46	23.98	16.54	7.44
160	46.54	26.88	18.32	8.56
170	49.44	29.79	20.07	9.72
180	52.16	32.70	21.78	10.92
190	54.72	35.59	23.44	12.14
200	57.15	38.45	25.07	13.39
210	59.43	41.30	26.65	14.65
220	61.60	44.11	28.19	15.92
230	63.66	46.90	29.69	17.21
240	65.63	49.65	31.15	18.50
250	67.52	52.37	32.56	19.80
260	69.33	55.05	33.94	21.11
270	71.09	57.70	35.29	22.41
280	72.78	60.32	36.60	23.72
290	74.42	62.90	37.87	25.03
300	76.00	65.45	39.12	26.33
310	77.54	67.97	40.33	27.64
320	79.05	70.45	41.52	28.93
330	80.53	72.91	42.68	30.23
340	82.00	75.33	43.81	31.52
273.15	71.63	58.53	35.70	22.83
298.15	75.71	64.98	38.89	26.09

Table 6. Experimental heat capacities of magnesite crystals from Brazil. Values have been corrected to the composition $MgCO_3$. Values are listed for a sample mass of 84.314 g.

Temp.	Heat capacity	Temp.	Heat capacity	Temp.	Heat capacity
K	$J \cdot mol^{-1} \cdot K^{-1}$	K	$J \cdot mol^{-1} \cdot K^{-1}$	K	$J \cdot mol^{-1} \cdot K^{-1}$
Series 1		Series 2		Series 3	
338.9	81.61	468.1	94.74	537.7	101.8
348.9	82.94	478.1	95.63	547.6	102.9
358.8	84.23	488.0	96.54	557.6	103.2
368.8	85.44	498.0	97.27	567.5	103.8
378.7	86.72	507.9	97.95	577.5	104.7
388.6	88.08	517.8	99.00	587.4	105.7
398.6	89.20	527.8	99.75	597.3	105.7
408.5	90.30	537.7	100.4	607.3	106.5
418.5	91.27	547.6	101.3	617.2	106.9
428.4	92.43	557.6	102.0	627.2	107.0
438.3	93.48	567.5	102.7	637.1	107.9
448.3	94.60	577.5	103.6	647.0	108.3
458.2	95.53	587.4	104.4	657.0	108.7
468.1	96.44	597.3	105.0	666.9	108.9
478.1	97.30	607.3	105.1	675.8	110.0
487.0	98.28	616.2	105.9		
497.0	99.12				

Table 7. Experimental heat capacities of $YBa_2Cu_3O_{6.9}$ corrected for curvature. Values are listed for a sample mass of 664.594 g.

Temp.	Heat capacity	Temp.	Heat capacity	Temp.	Heat capacity
K	$J \cdot mol^{-1} \cdot K^{-1}$	K	$J \cdot mol^{-1} \cdot K^{-1}$	K	$J \cdot mol^{-1} \cdot K^{-1}$
Series 1		Series 4		Series 7	
8.24	0.218	112.59	154.5	85.11	117.1
9.31	0.439	118.04	161.2	86.26	119.1
10.35	0.546	123.14	167.5	87.42	121.1
11.58	0.787	128.30	173.8	88.60	122.6*
12.98	1.215	133.50	179.9	89.82	122.8
14.44	1.820	138.63	185.8	91.05	124.5
16.08	2.715	143.72	191.4	92.27	125.7
17.90	3.857	148.78	197.2	93.48	127.3
19.88	5.522	153.80	201.4	94.68	128.9
22.10	7.464	158.80	205.0	95.89	131.0
24.58	9.844	163.77	210.6	97.09	131.7
27.34	13.18	168.72	215.0	98.29	134.5
30.41	18.12	173.65	219.2		
33.86	23.20	178.56	223.0	Series 8	
37.74	30.37	183.46	226.8		
42.07	38.22	188.34	230.6	55.56	70.55
46.91	47.61	193.23	234.4	60.56	83.03*
52.30	59.89	198.11	237.8	64.70	91.37
58.16	78.37*			69.35	94.02*
64.28	90.42	Series 5		74.78	99.07
70.50	94.52*			79.96	107.6
76.62	102.1	203.31	241.1	85.07	116.6
82.43	111.9	208.63	245.0		
88.03	121.2*	213.60	247.3	Series 9	
93.62	127.9	218.60	250.5		
99.19	136.0	223.48	253.1	56.64	73.67
104.64	143.6	228.40	255.4	57.57	78.74
110.00	150.8	233.38	258.4	58.51	82.32
115.29	157.8	238.39	261.7	59.57	79.57
120.51	164.2	243.42	262.9	60.65	82.33
		248.47	265.0	61.71	85.32
Series 2		250.53	267.3	62.77	87.32
		258.61	269.6	63.83	89.39
81.25	110.1	263.74	271.5	64.89	91.13
83.46	113.8	268.92	274.0	65.94	93.08
85.41	116.8			67.00	94.41
87.47	120.7	Series 6		68.04	95.17
89.68	123.1*			69.09	94.46
91.88	125.4	269.03	273.0	70.13	93.25
94.06	128.7	274.54	275.6		
96.24	131.7	279.66	277.4		
98.40	135.3	284.80	279.0		

Table 7. Continued.

Temp.	Heat capacity	Temp.	Heat capacity	Temp.	Heat capacity
K	$J \cdot mol^{-1} \cdot K^{-1}$	K	$J \cdot mol^{-1} \cdot K^{-1}$	K	$J \cdot mol^{-1} \cdot K^{-1}$
Series 3		Series 6		Series 10	
		289.93	281.6	71.31	93.84
84.31	115.8	295.05	283.8	72.39	95.22
85.34	117.4	300.16	285.5	73.34	96.88
86.33	118.8	305.26	286.8	74.29	98.49
87.37	120.8	310.35	288.6	75.31	100.2
88.47	122.1	315.43	290.3	76.32	102.1
89.57	122.2	320.49	291.8	77.32	103.3
90.66	123.9	325.53	293.3	78.34	104.5
91.75	124.9	330.57	294.2	79.36	107.2

* Enthalpy measurement

Table 8. Experimental heat capacities of $BiCaSrCu_2O_{6+x}$ corrected for curvature. Values are listed for a sample mass of 559.7688 g.

Temp.	Heat capacity	Temp.	Heat capacity	Temp.	Heat capacity
K	$J \cdot mol^{-1} \cdot K^{-1}$	K	$J \cdot mol^{-1} \cdot K^{-1}$	K	$J \cdot mol^{-1} \cdot K^{-1}$
Series 1		Series 3		Series 5	
301.53	234.1	14.98	4.148	112.29	127.7
307.33	235.6	16.67	5.392	117.94	133.6
312.70	237.2	18.54	6.918	123.63	139.2
318.08	237.9	20.63	8.856	129.44	144.8
323.52	240.1	22.95	11.15	134.90	149.8
328.96	241.8	25.54	13.92	140.32	154.7
		28.45	17.29	145.70	159.1
Series 2		31.72	21.43	151.03	163.5
		35.39	26.44	156.35	167.5
52.12	50.77	39.18	31.52	161.65	171.5
57.10	58.23	42.35	36.57	166.93	175.4
61.22	64.35	44.86	40.14	172.21	179.1
65.75	70.69	47.17	43.41	177.49	182.6
70.97	78.11	49.35	46.66	182.77	185.9
75.95	84.82	51.42	49.76	188.07	189.2
80.84	90.68	53.45	52.84	193.38	192.2
85.61	96.83			198.71	195.4
90.38	102.9	Series 4		204.09	198.2
95.19	108.2			209.50	201.2
99.93	114.2	80.66	90.66	214.97	203.6
104.59	119.6	82.54	93.19	220.53	206.1
109.18	124.6	84.30	95.62	226.24	208.6
113.71	129.3	86.13	97.76	232.11	210.9
118.19	133.9	87.90	99.83	238.12	213.3
122.62	138.2	89.74	102.4	244.21	215.4
127.00	142.6	91.65	104.4	250.35	217.5
131.36	146.7	93.55	106.7	256.51	219.7
135.70	150.6	95.44	109.5	262.70	221.9
140.00	154.5	97.32	111.8	268.94	224.1
		99.19	113.9	275.19	226.3
Series 3		101.05	115.9	281.42	228.3
		102.90	117.5	287.64	230.4
7.91	0.9740	104.73	119.5	293.84	232.7
8.96	1.236	106.55	121.7	300.01	234.5
9.84	1.546	108.36	123.7	306.17	235.8
10.84	1.840				
12.12	2.463				
13.47	3.179				

Table 9. Specific heat of 321 stainless steel made in one series.

T K	Cp $J \cdot g^{-1} \cdot K^{-1}$	T K	Cp $J \cdot g^{-1} \cdot K^{-1}$
53.63	0.103	207.61	0.427
59.90	0.126	213.05	0.431
64.56	0.145	218.47	0.434
68.63	0.163	223.89	0.439
72.22	0.177	229.32	0.442
75.60	0.190	234.77	0.446
78.92	0.202	240.22	0.448
82.18	0.213	245.65	0.451
85.44	0.224	253.86	0.452
92.42	0.246	256.55	0.457
97.40	0.260	261.77	0.459
102.65	0.275	267.00	0.463
108.07	0.289	272.39	0.465
113.89	0.303	277.78	0.467
119.66	0.316	283.14	0.469
125.38	0.327	288.49	0.472
130.95	0.338	293.83	0.474
136.18	0.347	300.00	0.476
141.50	0.355	306.90	0.479
147.08	0.364	312.52	0.481
152.66	0.372	305.09	0.477
158.21	0.379	310.07	0.479
163.75	0.386	315.16	0.482
169.30	0.392	320.26	0.483
174.81	0.398	325.51	0.485
180.31	0.404	330.75	0.487
185.79	0.409	335.98	0.488
191.26	0.414	341.20	0.490
196.71	0.419	346.42	0.492
202.16	0.423	351.63	0.494

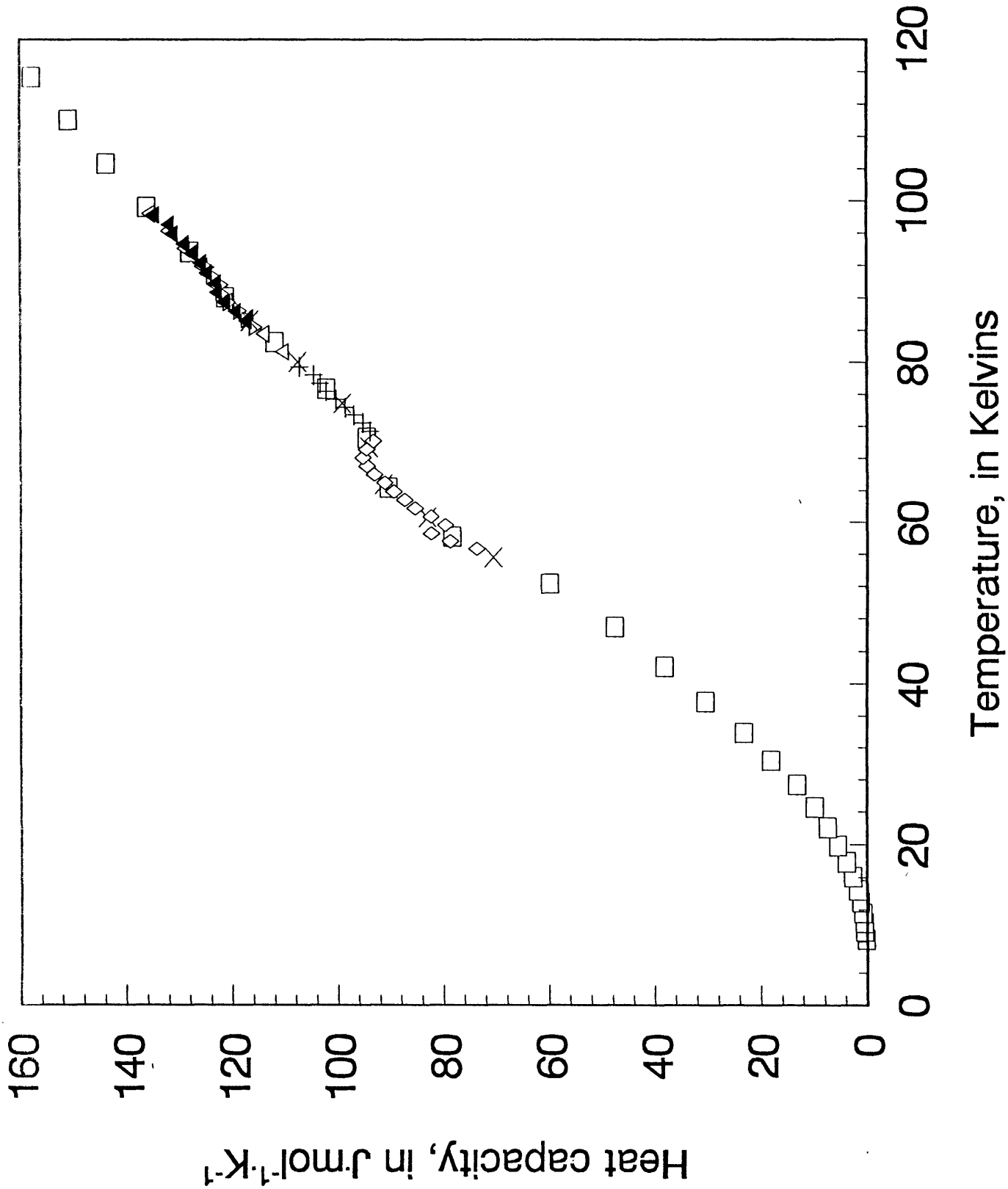

Figure 1. Experimental molar heat capacities of the high-temperature superconductor $YBa_2Cu_3O_{6+x}$ to 120 K. The symbols represent the various measurement series: open square - Series 1; X - Series 8; open diamond - Series 9; plus - Series 10; open triangle - Series 2; inverted open triangle - Series 3; and filled triangle - Series 7.

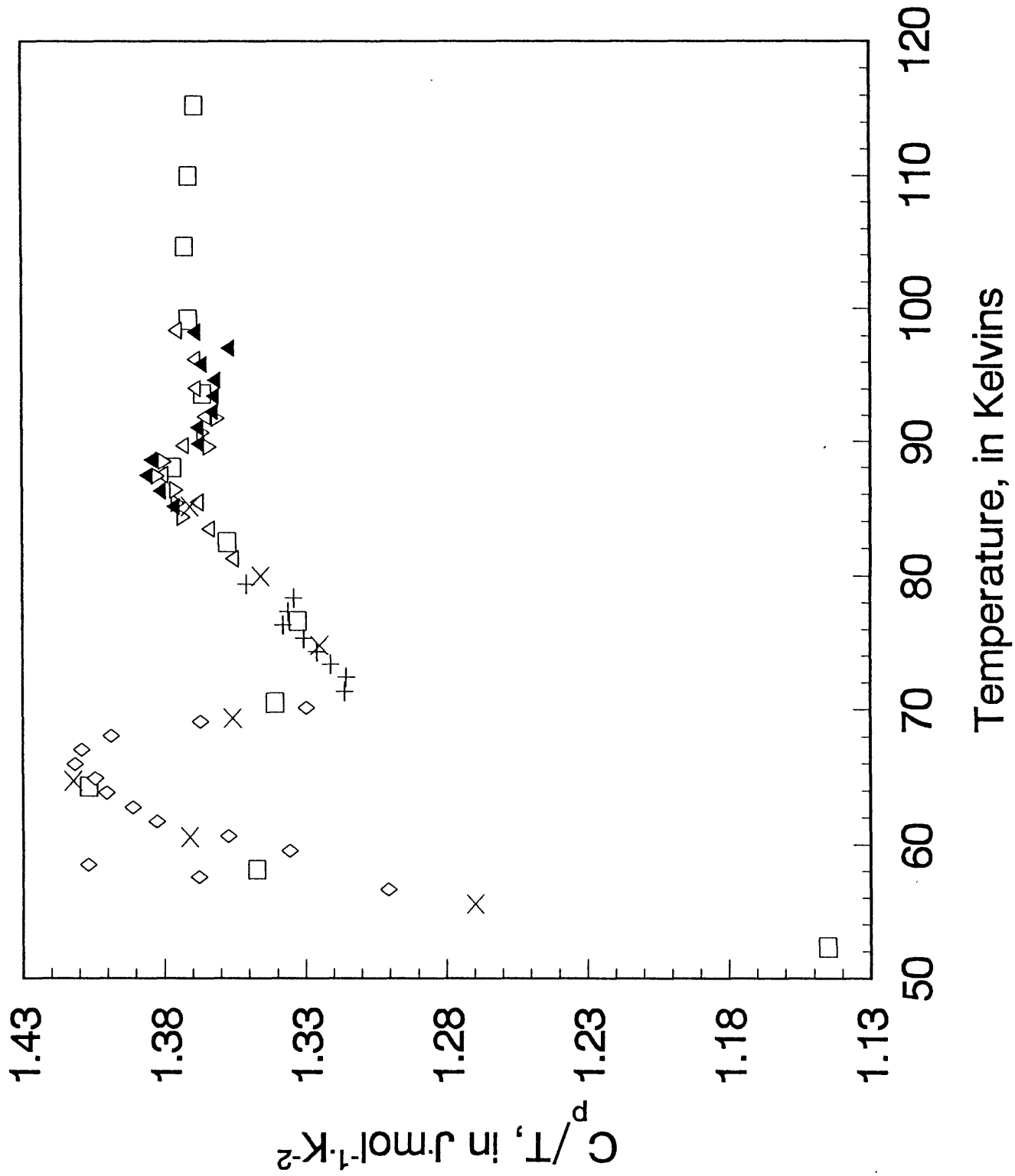

Figure 2. Molar heat capacities (as C_p/T) of $YBa_2Cu_3O_{6+x}$ showing the anomalous behavior in the temperature interval of 50 to 120 K. Symbols are described in the caption for Figure 1.

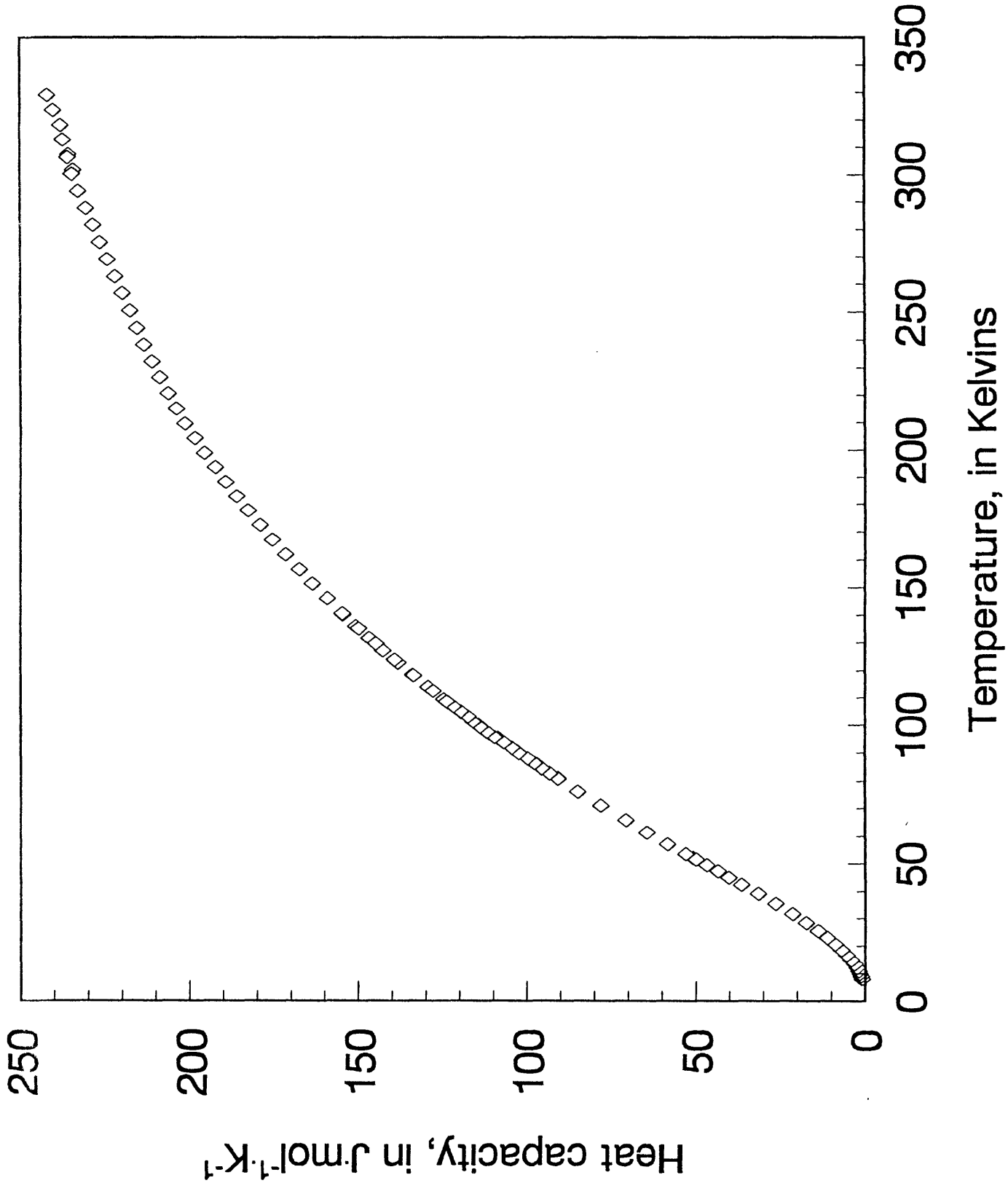

Figure 3. Experimental molar heat capacities of the high-temperature superconductor $BiCaSrCu_2O_{6+x}$.

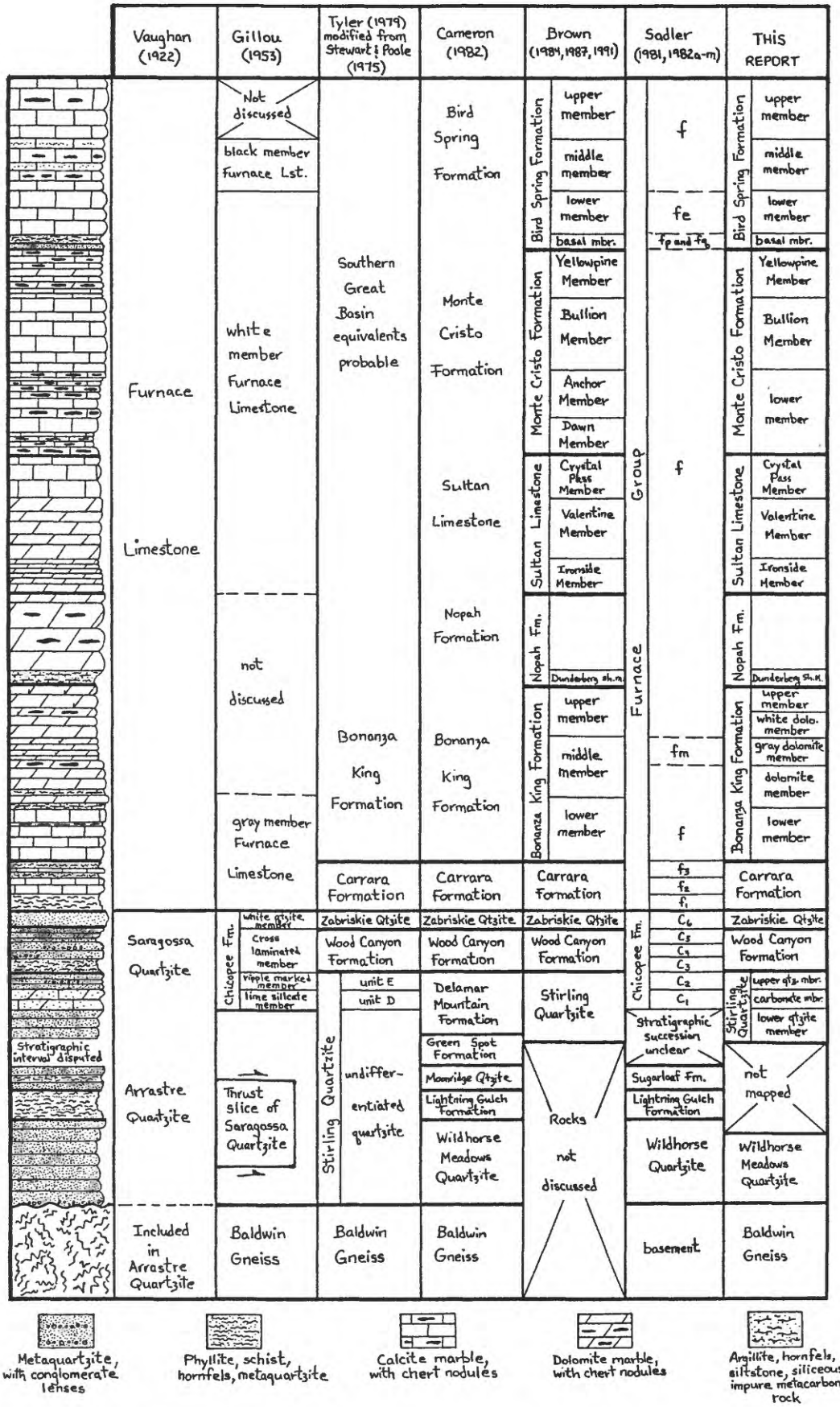

Figure 1.--History of stratigraphic classification of Proterozoic and Paleozoic metasedimentary rocks in the north-central San Bernardino Mountains.